IIBCC 2010
International Inorganic-Bonded Fiber Composites Conference

THE FRACTURE STRENGTH OF FIBRE-CEMENT CORRUGATED SHEETS: A STATISTICAL APPROACH USING WEIBULL ANALYSIS

KRUNOSLAV VIDOVIČ[1], MILAN AMBROŽIČ [2], <u>KRISTOFFER KRNEL</u> [3], TOMAŽ KOSMAČ[2] and STEPHEN AKERS[4]

[1]*Esal d.o.o. Anhovo, Vojkova 9, SI-5210 Deskle, Slovenia;* [2] *Faculty of Natural Sciences and Mathematics, University of Maribor, Koroška 160, SI-2000 Maribor;* [3]*Jožef Stefan Institute, Jamova 39, SI-1000 Ljubljana, Slovenia;* [4] *Eternit (Schweiz) AG, CH-8867 Niederurnen, Switzerland*

ABSTRACT

The breaking load and the breaking moment during transversal and longitudinal loading of fibre-cement profiled (corrugated) sheets were measured on products manufactured on an industrial Hatschek machine, and the corresponding bending strengths were calculated. The influence of two processing parameters, i.e., the pressure applied to the green sheet directly during the manufacture and the content of the reinforcing organic fibres within the portland cement matrix, on the fracture strength of the products was studied and statistically analyzed assuming Weibull statistics. The Weibull parameters were compared for different fabrication conditions. While the fibres content influences considerably the Weibull modulus for both transversal and longitudinal loading, there is no correlation between the shaping pressure and Weibull modulus.

KEYWORDS:

Cement; Fibre reinforcement; Bending strength; Weibull statistics.

INTRODUCTION

In recent years there have been numerous successful investigations relating to the development of fibre-cement composites using various organic or synthetic fibres (Studinka 1989; Savastano et al. 2003; Coutts 2005; Agopyan et al. 2005; Ma et al. 2005; Peled and Mobasher 2005). The candidate fibres for such composites need to meet several requirements, such as high strength and appropriate elastic modulus, chemical, temperature and dimensional stability, resistance to an alkaline environment, the appropriate morphology and compatibility with the cement matrix, good dispersion properties in an aqueous cement slurry, and long-term durability. One of the synthetic fibre types with appropriate properties for use in fibre-cement composites is polyvinyl alcohol (PVA) and it is used in our manufacture of corrugated sheets. However, new composite materials have to be tested rigorously using classical mechanical tests as well as various accelerated ageing tests to predict the long-term behaviour of the products under severe climatic conditions (Akers and Studinka 1989; Akers 1989; Purnell and Beddows 2005). Different testing requirements should be applied to different fibre-cement products, e.g., profiled (corrugated) roofing sheets, facades, pipes, etc., and also with respect to different climatic conditions.

Improvements and/or cost reductions relating to the fibre-cement fabrication process and the quality of the final products (in our case corrugated roofing sheets) can be achieved by varying different processing parameters (Ma et al. 2005; Vidovič et al. 1996; Negro et al. 2005; Negro et al. 2006; Beaudoin 1990). With regard to the fibres, their type, volume fraction and length are typical parameters that influence the mechanical properties (Ma et al. 2005). It is also known that increasing the volume fraction of the reinforcing fibres increases the composite tensile strength because of the partial transfer of the load from the cement

matrix to the fibres. However, at very large fibre contents some detrimental effects occur, such as increased porosity and a weaker interface between the fibres and the matrix; in addition, the production costs are increased. With regard to other processing parameters, the pressure used to shape the green sheet products is of great importance. To optimize the production the influence of variable processing parameters on the mechanical properties of the composite materials/products should then be measured and analyzed. Usually, mechanical tests are performed on laboratory-made samples with a simple geometry, rather than on final products from serial production.

The measured strengths in typical mechanical tests for many brittle and quasi-brittle materials result in a Weibull statistical distribution (Weibull 1949; Weibull 1951; ReliaSoft 1992; Kosmač et al. 1999; Setien 2005; Lewis et al. 2005). This statistical distribution has been widely used in many fields, with many examples from the literature given (Reliasoft 1992). Weibull statistics have also been used in civil engineering (Anton et al. 1998; Toutanji 1999; Caliskan 2003; Li et al. 2003; Huang and Cheng 2004; Cooke 2005). Usually, simple 2-parameter Weibull statistics are used, although in many cases the 3-parameter Weibull statistics or the Weibull statistics corresponding to two or more different modes of fracture works better (Reliasoft 1992; Li et al. 2003).

This investigation has the aim of checking the relevance of the two of the production parameters with regard to the strength of fibre-cement corrugated roofing sheets, i.e., the volume fraction of the fibres and the shaping pressure on the green sheet. The experiments were performed on industrial products in order to avoid the difficult translation of know-how from a research laboratory to industry. In this article the results on measurements/calculations of four mechanical properties of the corrugated roofing sheets are presented: the breaking force during transversal loading, the breaking bending moment during longitudinal loading, and the calculated bending strengths for transversal and longitudinal loadings. The experimental data were fitted to the 2-parameter Weibull probability distribution function. The aim of this paper is to show that the 2-parameter Weibull statistics can be used successfully in this case and that it reveals significant differences in the statistical parameters when the production parameters are varied. Some evidence is also given for the influence of the alignment of PVA fibres on the difference in the effective bend strength of the material for transversal and longitudinal loading, respectively.

EXPERIMENTS AND STATISTICAL PROCEDURE

Materials and processing

The mix composition of the final profiled sheet material (after 21 days of maturing) is given in volume fractions as follows: 40% of hydrated portland cement, which represents the matrix; 30% of air captured in pores; 12% of water; 11% of inorganic additives, such as fillers and pigments; 5% of processing cellulose fibres; and 2% of reinforcing PVA fibres.

The manufacturing process for the corrugated sheets used in this work is essentially the Hatschek procedure (Studinka 1989). All the material components are first dispersed and homogenized in water, producing a highly diluted suspension. In the filtration process a filter cake is formed on rotating sieve cylinders, and it is then transported by the felt conveyer to the forming drum. When the desired thickness of deposited material on the drum is achieved, it is cut and transported on a conveyer belt for corrugating and pressing, which is followed by primary maturing of the product at an elevated temperature. Finally, the products are matured for 21 days under ambient conditions in a closed warehouse.

The mechanical testing was performed on standard products from production, i.e., a fibre-cement corrugated roofing sheet, referred to as V5, with the following dimensions (Fig. 1): width $W = 920$ mm, length $L = 1250$ mm, corrugation pitch $P = 177$ mm, corrugation height $H = 51$ mm. The typical thickness, T, of the V5 sheet is between 5.95 mm and 6.20 mm.

In the first part of the experiment the mass fraction, c_f, of the PVA and cellulose fibres was varied in the initial products. For three different material compositions the mass fractions of the fibres with respect to the total mass of solid components (without water and air) were as follows: $c_f = 5.4\%$, 5.7% and 6.1%,

respectively; the remaining portion being the cement, additives and fillers. The mass ratio of the reinforcing PVA fibres to the processing cellulose fibres was 1:2 in all three cases. The corrugation shaping pressure, p_s, of the hydraulic press during the shaping of the V5 sheets was 10 MPa. In the second part of the experiment the shaping pressures p_s = 8 MPa, 9 MPa and 10 MPa, respectively, were used, keeping the mass fraction of the fibres at 6.1%. The reason for the relatively narrow span of the chosen variable parameters was the following. In the ordinary industrial production process we have c_f = 6.1% and p_s = 10 MPa. As already mentioned, the trial change of parameters was made in massive serial production with many products where we could not afford changing the parameters too widely, with the risk of degrading the quality of the products to the degree that they have to be discarded. On the other hand, even slight reducing the PVA-fibres content, for instance from 6.1% to 5.4% without measurable degradation of mechanical properties, would lower the production cost.

Measurement of the mechanical properties

For the determination of the mechanical properties of the V5 sheets the methods prescribed by the European standard EN 494 were used (EN 2004). Before the mechanical tests were conducted the test sheets were soaked in water for 24 h and then briefly dried according to the standard. The focus for the discussion in this paper was the measurement of the breaking force (transversal loading) and the bending moment (longitudinal loading); in addition, the bending strengths for both the transversal and longitudinal loadings were calculated. For these measurements a BP-10 laboratory press-machine (Walter+Bai AG, Switzerland), with the measuring scales 2 kN and 10 kN, and equipped with the corresponding software, was used. The geometry of the transverse and longitudinal loadings, according to the EN 494 standard, is shown in Fig. 1. While the breaking force (load) was measured directly for both types of loading (transversal and longitudinal), the three remaining properties were calculated from the breaking force and the geometrical parameters of the test.

TRANSVERSAL LOADING: According to EN 494 this is essentially a 3-point bending test (Fig 1a). The width of the horizontal transverse supports is 50 mm, and the inner span is 1100 mm. On the upper side of the sheet a transverse loading beam with a width of 230 mm is placed symmetrically with respect to the supports. It is necessary to insert 10-mm-thick strips of soft material (possibly felt) between the sheet, the supports and the loading beam. The breaking load (force) is usually defined per unit width of the sheet, but in this case a constant width W = 920 mm was used; therefore, the results for the breaking force are expressed in Newtons (N) for the actual width of 920 mm (Table 1). The transversal breaking force (load) is denoted by F_T, where the index T refers to the transversal loading.

LONGITUDINAL LOADING: This is again a 3-point bending test, but with the supports in the longitudinal directions of the sheet (in Fig. 1b, one of the possible variants is shown). A sample of the sheet, at least L' = 300 mm long, should be cut for the longitudinal loading test. The supports should be rounded, while a soft material strip (possibly felt) should be used for the contact between the sheet and the loading beam, as is the case for the transversal loading. The span S between the supports is determined by the corrugation pitch. The bending moment M_L at the moment of rupture is expressed per unit length L' of the test piece and is given by the expression:

$$M_L = \frac{FS}{4L'}$$

(1)

where F is the breaking load. The index L in the term M_L refers to the bending moment for longitudinal loading, and the moment itself as a vector has the longitudinal direction, i.e., parallel to the corrugations.
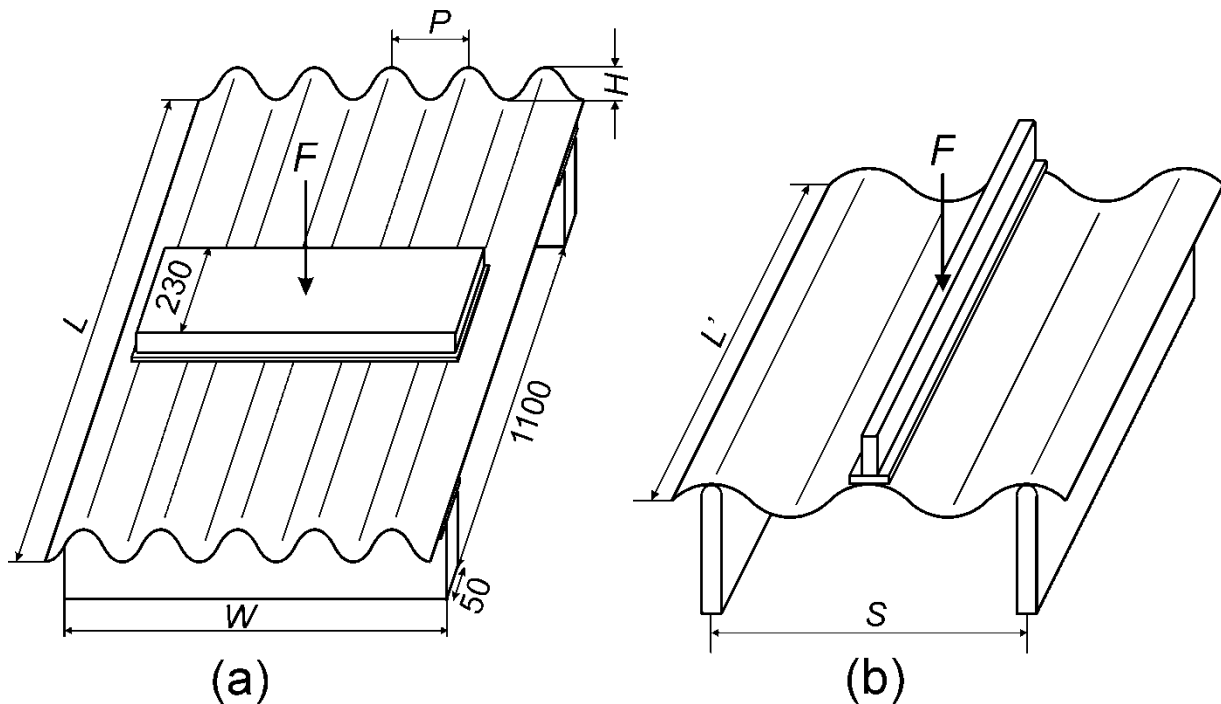
Fig. 1 The geometry of transverse (a) and longitudinal (b) loading according to the European standard EN 494. Lengths are given in millimetres.

A comment should be given why the force and the moment of force are relevant for the transversal and longitudinal bending loading according to the standard EN 494. In bending loadings in the tests and in everyday use it is the moment of force (and not the force itself) which determines when the sample/product breaks since the span between the supports is also relevant. While in the transversal loading the moment of force could be used as the criterion for the quality of the corrugated sheet the span between the supports is uniquely prescribed by the standard (Fig. 1) and thus the force can be simply used as a testing property. On the other hand, in the longitudinal loading, the span cannot be uniquely defined (the corrugation pitches differ for different products) and so the loading moment must be kept as a standard.

TRANSVERSAL AND LONGITUDINAL BENDING STRENGTHS: While the force F_T and the moment M_L are the most interesting properties with regard to the application of the final V5 fibre-cement products, rather than the material bending strength, the latter is calculated and included in the discussions for comparison. For both the transversal and longitudinal loadings of the V5 sheets the calculation of the bending strengths, σ_T and σ_L, respectively, from the load at rupture and the geometric parameters of the sheet and the bending test is rather complicated, due to the geometry of the corrugated sheets. The problem of transversal loading is easier since the applied stress can be treated as uni-axial since the cross section of the sheet is uniform through its length, thus the main problem is calculating numerically the cross-section inertia moment for the given sheet profile. On the other hand, for longitudinal loading the direction of stresses varies according to the corrugations between the supports, and the entire stress analysis is necessary. Here special software developed by Eternit, Switzerland, was used to calculate the strengths from the input data (breaking load, type of loading, geometry and dimensions of the sheets). The formulas for the evaluation of the transversal bending strength can also be found in the DIN 274/1 standard (DIN 1972).

The relative measurement uncertainties were roughly as follows: 0.5% for the force, 0.1% or less for the length scales (other than the sheet thickness), and 1% for the sheet thickness. Since the relative uncertainties for multiplied or divided quantities are added together an estimate can be made of the relative uncertainties of M_L, σ_T and σ_L. Using Eq. (1) for the bending moment, we obtain its relative uncertainty: 0.5% + 2*0.1% = 0.7%. Calculations of the bending strengths scale with the factors/quotients F, L/L and T^2 (where F, L and T are the breaking force, the geometrical lateral dimensions and the sheet's average thickness, respectively),

thus the relative uncertainty of the strengths is 0.5% + 2*0.1% + 2*1% = 2.7%. The actual uncertainties may, however, be somewhat larger, due to misalignments and variability of the sheet thickness.

Statistical evaluation

It has been shown that for brittle ceramic materials at least 30 measurements of the mechanical strength are needed in order to obtain sufficiently reliable Weibull statistics (Quinn 1990). The fibre-cements behave as quasi-brittle materials in the bending test for which we have found no direct recommendations about the number of samples in the literature, thus facing the experience of ceramic materials we adopted the number of samples $N = 30$ samples for each set of processing parameters. The individual measurements were then statistically evaluated. First, the mean values and the standard deviations were calculated. Then the data were fitted to the 2-parameter Weibull statistics as follows.

Let the statistical variable be denoted by x (x being one of the measured/calculated quantities, F_T, M_L, σ_T, σ_L.) and let its failure probability function be $P(x)$, where the letter P refers to the probability. The function $P(x)$ is the probability of finding the value for the measured variable to be less than x. If we assume all possible values of x between zero and infinity, then at both limits, $P(0) = 0$, and $P(\infty) = 1$ holds. In the literature, this function can also be called the unreliability function (ReliaSoft 1992). In the case of 2-parameter Weibull statistics, $P(x)$ is equal to:

$$P(x) = 1 - \exp(-(\frac{x}{x_0})^m) \tag{2}$$

with the pair of Weibull parameters m and x_0. The dimensionless Weibull modulus, m, refers to the slope of the line in the special Weibull plot diagram (Reliasoft 1992), while the scale parameter x_0 determines its position, as shown in Fig. 3. Here, a rough sketch of the procedure is given to find the Weibull parameters; the reader can find details elsewhere (Reliasoft 1992; Ritter et al. 1981; Johnson 1951; Lloyd and Lipow 1962).

The N measured values x_i of the quantity x ($i = 1$ to N) are first sorted in increasing order. Then the value P_i is attributed to the i-th value x_i (P_i being independent of the value x_i) by solving the equation:

$$\sum_{k=i}^{N} \binom{N}{k} P_i^k (1-P_i)^{N-k} = 0.5 \tag{3a}$$

in accordance with the binomial distribution (Johnson 1951). This equation for P_i has to be solved numerically. Alternatively, a much simpler equation can be used, which leads to similar calculated values for P_i:

$$P_i = \frac{i - 0.3}{N + 0.4} \tag{3b}$$

Other simple formulas are also used in the literature, instead of Eqs. (3a) and (3b) (Reliasoft 1992; Li et al. 2003; Li et al. 1993; Wu et al. 2006). Using Monte Carlo simulations, Wu et al. showed that simple formulas like (3b) give slightly biased values of Weibull moduli, either too high or too low values; for instance, Eq. (3b) results in an about 5% underestimated value of m, for N between 15 and 50 (Wu et al. 2006). The ordered data pairs (x_i, P_i) for $i = 1$ to N are finally fitted to the function (2) by the usual fitting procedures, in order to obtain the Weibull parameters m and x_0, as shown in Fig. 3. Because there is a limited number of measurements (in this case $N = 30$) the Weibull parameters obtained need not be equal to their true values for a statistical assessment of many samples; rather, these are estimated values of m and x_0. Knowing the estimated Weibull parameters one can re-evaluate various statistical parameters, for instance, the mean value of the variable x and its standard deviation, and compare the calculated values with the values obtained from experimental data.

Once the parameters of the Weibull statistics are obtained the reliability of their estimated values should be evaluated. This is usually done with the help of the Fisher matrix of the system (Lloyd and Lipow 1962). One can then predict with some confidence level *CL*, say 90%, that the actual value of the parameter lies within some interval. ReliaSoft's commercial computer program package Reliasoft-Weibull++ for the computation and visualization of the statistical distribution was used (Reliasoft 1992).

RESULTS AND DISCUSSION

Typical deflection-load curves for transversal and longitudinal loading are schematically sketched in Figs. 2. Two typical points on the curves are the limit of proportionality (LOP) and the modulus of rupture (MOR), where the load reaches its maximum value. At LOP the first sign of matrix cracking is detected. Between LOP and MOR multiple matrix cracking occurs together with fibre pull-out and fibre fracture. After MOR the fibre pull-out and fibre fracture is continued and is believed to gradually become the dominant failure mechanism. The difference in the shape of deflection-load curves for both types of loading (rather complicated curve with more maxima for transversal loading in comparison to simple curve for longitudinal loading) is attributed to the cascade failure for transversal loading (not all of the corrugations fail simultaneously). Since the deflection-load curves are shown in arbitrary units in order to directly compare the curves for two physically different quantities (force and moment of force), we mention here some numerical data for the reader's evidence. The MOR for the transversal loading is approximately at the average deflection of 40 mm (the actual span of values is between 20 mm and 70 mm) and the force between 5 kN and 6 kN. The MOR for the longitudinal loading is at the deflection between 20 mm and 30 mm and the moment of force per unit length between 90 N m/m and 100 N m/m.

The average values and the standard deviations (in parentheses) of the quantities F_T, M_L, σ_T and σ_L for $N = 30$ samples for each group are shown in Table 1. The standard deviations for all quantities are of the order of 10% of their mean values, which is much larger than the measurement uncertainties mentioned in subsection Measurement of the mechanical properties. It has been shown by Monte Carlo simulations that the influence of measurement errors on the statistics may be ignored unless they become comparable to the natural deviations of the measured quantities due to intrinsic differences between the samples (Ambrožič and Vidovič 2007).

It can be seen from Table 1 that while the mean values of all the quantities increase with increasing fibre content, the shaping pressure has a significant effect on the properties only during longitudinal loading. It is also evident that although the given composition and pressure are the same ($c_f =6.1\%$, $p = 10$ MPa) for the 3rd and 6th data rows in the table, the measured results are not completely equal; but the results are similar anyway, indicating a good consistency with control parameters. There was a 3-month period between the production and measurement of the mechanical properties of the series corresponding to the 3rd and 6th rows.
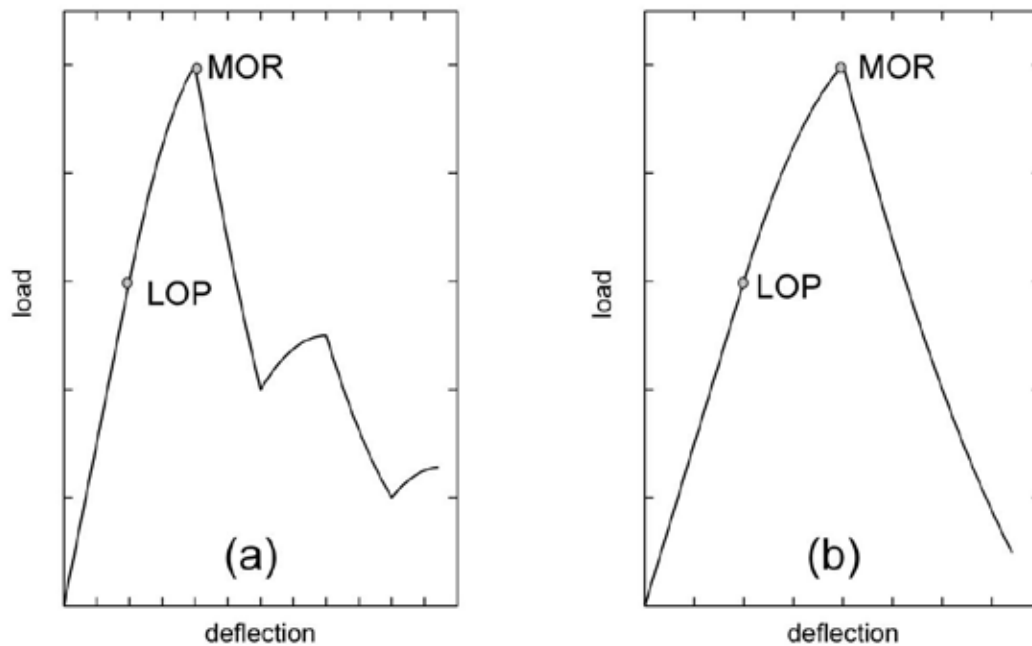
Fig. 2 Typical schematic deflection-load curve for transversal (a) and longitudinal (b) loading

Table 1. The dependence of the mechanical properties of the V5 sheets on the mass fraction of fibres c_f and the shaping pressure p_s: average values and standard deviations (in parentheses).

Data row	c_f (%)	p_s (MPa)	F_T (N)	M_L (N m/m)	σ_T (N/mm^2)	σ_L (N/mm^2)
1	5.4		5056 (589)	92.8 (10.6)	19.16 (1.78)	13.31 (0.86)
2	5.7	10	5550 (548)	99.2 (11.4)	20.95 (2.03)	15.02 (1.48)
3	6.1		5794 (395)	104.3 (9.1)	22.34 (1.30)	16.78 (1.02)
4		8	5682 (485)	85.0 (8.5)	21.88 (1.60)	13.36 (1.12)
5	6.1	9	5508 (375)	91.9 (7.6)	20.97 (1.32)	15.29 (1.05)
6		10	5652 (441)	102.9 (11.1)	21.74 (1.53)	16.62 (1.06)

The estimated Weibull moduli, *m,* and the scale parameters ($x_0 \rightarrow F_{T0}, M_{L0}, \sigma_{T0}$ and σ_{L0}) are shown in Tables 2a-2d, together with the correlation coefficient, ρ, which indicates how the experimental data fit to the 2-parameter Weibull statistics. The value $\rho = 1$ means an exact (idealized) fit. It can be seen that the correlation coefficient is in most cases almost equal to 1, indicating a good fit of experimental data to the 2-parameter Weibull statistics. The Weibull moduli are of the order of 10, comparable to brittle ceramic materials. For comparison with ceramic materials and with our results for corrugated roofing sheets, Huang and Cheng obtained Weibull moduli for the measured fracture toughness mostly between 7 and 10 for foamed alumina cements of different relative densities (Huang and Cheng 2004), while Li et al. reported moduli of about 7 and 12 for the body and surface crack mode, respectively, in their bimodal Weibull statistical distribution for the strength of their concrete specimens (Li et al. 2003).

Table 2a The estimated Weibull statistical parameters for the force F_T

Data row	c_f (%)	p_s (MPa)	m	F_{T0} (N)	ρ
1	5.4		9.9	5310	0.986
2	5.7	10	11.6	5793	0.948
3	6.1		17.2	5970	0.976
4		8	13.6	5896	0.974
5	6.1	9	17.1	5677	0.973
6		10	14.9	5849	0.961

Table 2b The estimated Weibull statistical parameters for the moment M_L

Data row	c_f (%)	p_s (MPa)	m	M_{L0} (N m/m)	ρ
1	5.4		9.9	97.5	0.983
2	5.7	10	10.1	104.2	0.931
3	6.1		13.4	108.3	0.985
4		8	11.6	88.8	0.952
5	6.1	9	13.9	95.4	0.938
6		10	10.8	107.7	0.976

Table 2c The estimated Weibull statistical parameters for the bending strength σ_T

Data row	c_f (%)	p_s (MPa)	m	σ_{T0} (N/mm^2)	ρ
1	5.4		12.3	19.95	0.978
2	5.7	10	11.7	21.87	0.935
3	6.1		19.9	22.93	0.983
4		8	15.8	22.60	0.982
5	6.1	9	18.4	21.57	0.966
6		10	16.6	22.42	0.976

Table 2d The estimated Weibull statistical parameters for the bending strength σ_L

Data row	c_f (%)	p_s (MPa)	m	σ_{L0} (N/mm^2)	ρ
1	5.4		17.8	13.70	0.962
2	5.7	10	11.8	15.67	0.969
3	6.1		18.7	17.26	0.936
4		8	13.9	13.86	0.948
5	6.1	9	16.3	15.79	0.892
6		10	18.1	17.11	0.960

The following discussion will be mainly focused to the Weibull parameters relating to the quantities F_T and M_L. The modulus m increases with the mass fraction of fibres c_f (but more significantly for F_T), while there is no evident correlation between m and the shaping pressure, p_s. Similarly, the scale parameters F_{T0} and M_{L0} evidently increase with increasing c_f, but for increasing pressure p_s only an increase of M_{L0} is evident.

However, to be certain of the explanations given above, one needs to have information about the confidence of the estimated Weibull parameters, as well as the mean values and the standard deviation calculated either directly from the experimental data or from the Weibull parameters. Table 3 gives an example of the

boundary values of 90%-confidence level intervals (shortly 90%*CL* intervals) for both the Weibull parameters and the calculated mean value of the force F_T in the case of variable c_f and fixed $p_s = 10$ MPa, corresponding to the data in rows 1-3 in Tables 1 and 2a. For instance, the values $m = 7.9$ (LB = lower boundary value), 9.9 (EST = estimated value) and 12.5 (HB = higher boundary value) in the first row of Table 3 mean that the estimated value $m = 9.9$ (rewritten from Table 2a) fits the experimental data best, but there is a 90% probability that the actual (unknown) value of m lies within the interval $7.9 < m < 12.5$. Note that the estimated parameter is the geometrical (but not arithmetical) average of both boundary values of 90% CL intervals.

Table 3 Estimated values and 90%CL intervals for the Weibull parameters m and F_{TO}, and the corresponding calculated mean values $<F_T>$ for the transversal breaking force.

Data row	c_f (%)	M			F_{T0}			$<F_T>$		
		LB*	EST*	HB*	LB*	EST*	HB*	LB*	EST*	HB*
1	5.4	7.9	9.9	12.5	5142	5310	5483	4863	5050	5244
2	5.7	9.4	11.6	14.4	5632	5793	5959	5362	5545	5735
3	6.1	14.0	17.2	21.2	5857	5970	6086	5657	5789	5925

*LB = lower boundary value according to 90%-confidence level intervals

*EST = estimated value

*HB = higher boundary value according to 90%-confidence level intervals

The 90%CL intervals for m are relatively wide, typically about 40% of the estimated value. The 90%CL intervals for the scale parameters are about 5% of the estimated value, in accordance with Li et al. (1993). It should, however, be remembered that the relative differences in the estimated Weibull parameters are larger than the differences for scalar parameters for different processing parameters, as well. Therefore, with regard to both Weibull parameters, in some cases the 90%CL intervals for different processing parameters overlap and in some cases they do not. For instance, the 90%CL interval for m in the case $c_f = 6.1\%$ overlaps only slightly with the interval for $c_f = 5.7$ and is clearly distinct from the interval for $c_f = 5.4\%$.

The Weibull statistics for different cases from Table 2 are visualized in Figs. 3a-3d, which show the fitting of data pairs (x_i, P_i) to the $P(x)$ functional dependence. The horizontal and vertical scales of the diagram are arranged in order to present the $P(x)$ function as a straight line (solid lines in Figs. 3a-3d), where the larger Weibull modulus corresponds to the steeper line. The 90%*CL* intervals for the Weibull parameters are taken into consideration, so that each distribution line is surrounded by a pair of dashed lines, inside which most data points should lie. In Fig. 3a the $P(F_T)$ distributions are compared for $c_f = 5.4\%$ and 6.1% (both the 4th and 6th rows in Table 2a for the latter fibre content). Fig. 3b makes a similar comparison of the $P(M_L)$ statistics for $c_f = 5.4\%$ and 6.1%. Figs. 3c and 3d compare the statistics for F_T and M_L, respectively, for two different pressures: $p_s = 8$ MPa and 10 MPa. The Weibull moduli are similar for both pressures, but there is still an increase of the scale parameter in the case of M_L. Graphs for intermediate values of processing parameters, i.e., $c_f = 5.7\%$ in Figs. 3a and 3b, and $p_s = 9$ MPa in Figs 3c and 3d were not included to keep the diagrams clear.
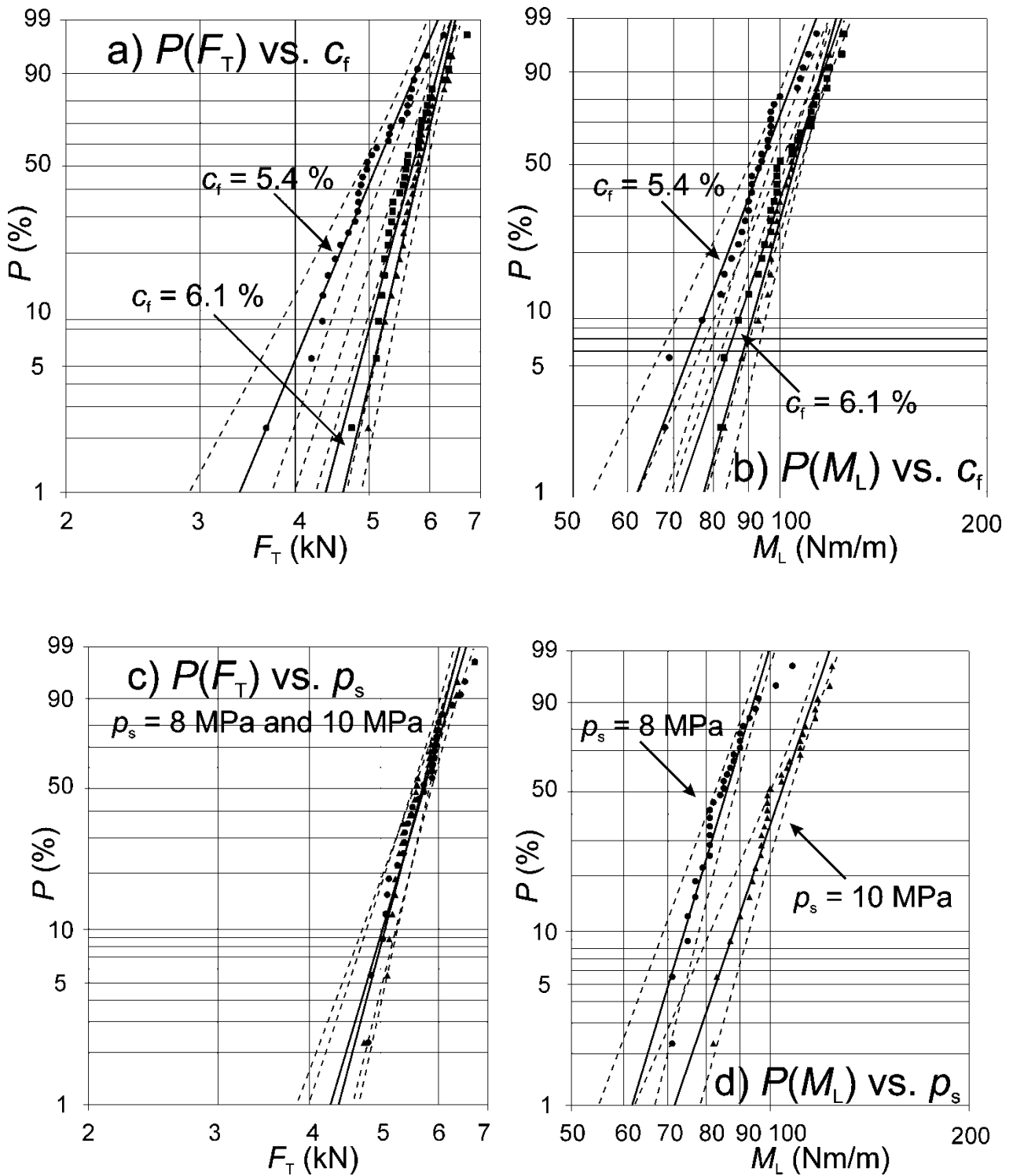
Fig. 3 Fitting of the $N = 30$ data pairs to the 2-parameter Weibull statistics: a) $P(F_T)$ for $c_f = 5.4\%$ (circles) and 6.1% (triangles and squares), rows 1, 3 and 6 from Table 2a, $p_s = 10$ MPa; b) $P(M_L)$ for $c_f = 5.4\%$ (circles) and 6.1% (triangles and squares), rows 1, 3 and 6 from Table 2a, $p_s = 10$ MPa; c) $P(F_T)$ for $p_s = 8$ MPa (circles) and 10 MPa (triangles), rows 4 and 6 from Table 2a; d) $P(M_L)$ for $p_s = 8$ MPa (circles) and 10 MPa (triangles), rows 4 and 6 from Table 2b.

The mean values of the transversal bending strengths are higher than for the longitudinal bending strengths. One of the main reasons for this is most probably the preferred orientation of fibres in the longitudinal direction of the V5 sheets (Cooke 2005), as shown in scanning electron microscope (SEM) microstructures on Figs 4a-4b. Fig. 4a shows a polished fibre-cement-sheet surface containing the production direction of the machine which is the longitudinal direction of the sheet while Fig. 4b is a cross-section perpendicular to that direction. It is clearly seen that the fibres (dark wavy lines) are preferably (although not completely) oriented in the sheet-longitudinal direction. A greater strength of the material when loading perpendicular to the orientation of the fibres compared to longitudinal loading was confirmed by bending tests on simple flat specimens removed from the production line before corrugation took place. As already mentioned the main failure mechanism is first cracking the cement matrix followed by pull-out and rupture of the reinforcing fibres. It is natural to expect that the pull-out and the rupture of PVA fibres is more pronounced in transversal loading compared to longitudinal loading. This expectation would need a quantitative verification, but nevertheless supports the findings from the bending test results that the contribution of the fibres to strength properties is obviously dependent on the preferential orientation of the synthetic fibres in particular. It needs also to be pointed out that although the synthetic fibres have the predominant contribution to strength properties, the cellulose fibres do provide additional strength to the products as well. Figs. 5a and 5b show the SEM pictures of the fracture surface of the sheet in transversal and longitudinal loading, respectively.
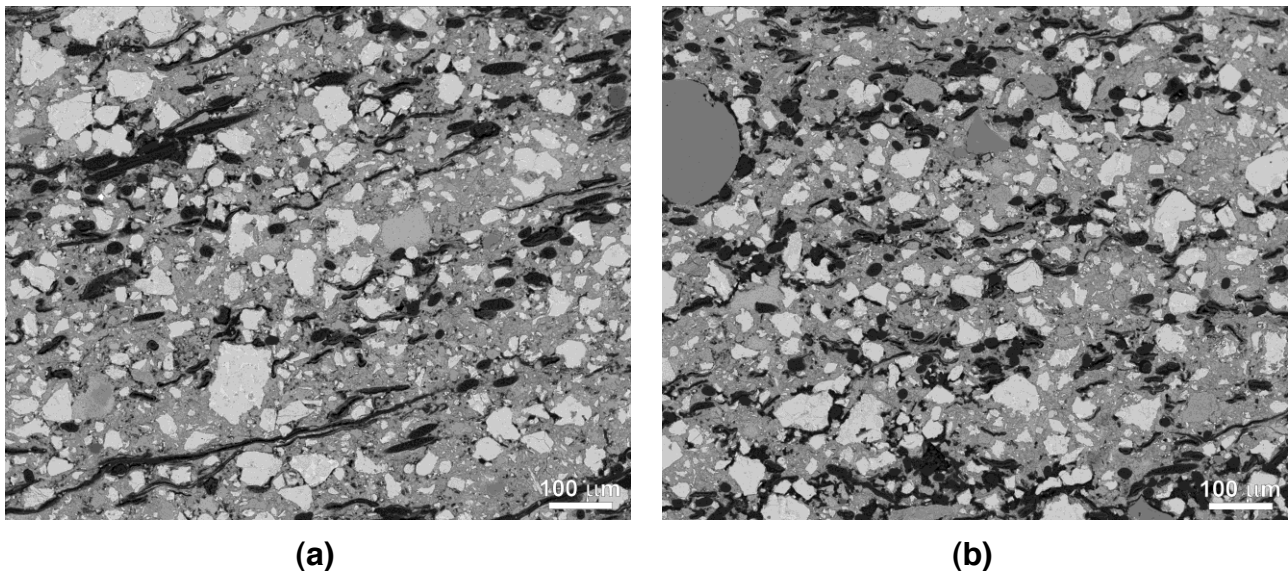

(a)   (b)

Fig. 4 SEM micro-structure of the polished surface of the PVA-fibre cement corrugated sheet containing the longitudinal direction of the sheet (a) and perpendicular to it (b).
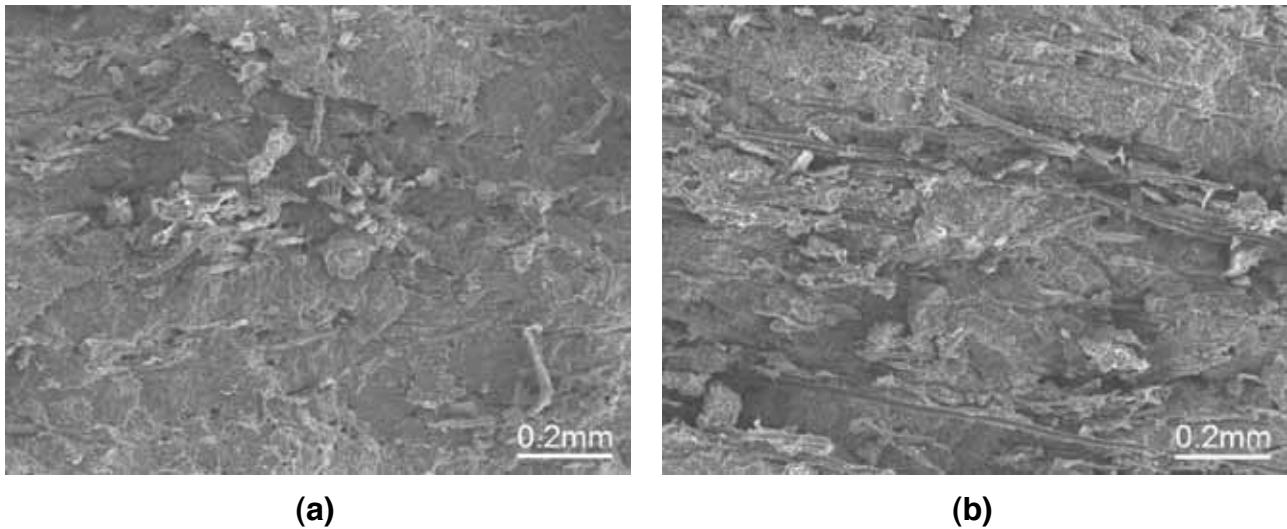
(a)   (b)

Fig. 5 SEM micro-structure of typical fracture surfaces of the sheets tested in the transversal (a) and the longitudinal (b) loading direction.

CONCLUSIONS

A study of the statistical distribution of repeated measured values of some mechanical properties of V5 corrugated roofing sheets showed that the measurements can be fitted well to the 2-parameter Weibull statistical distribution. The fitted Weibull moduli are high, and they show a correlation with the volume fraction of the reinforcing and processing fibres in the cement matrix. Higher volume fractions result in higher strength of the products. There is no conclusive correlation with the shaping pressure for the range of pressures under consideration in the present study. The statistical distributions can be conveniently visualized in special Weibull plots, where the failure probability function is represented as a straight line, with the Weibull modulus determining its slope.

ACKNOWLEDGEMENT

REFERENCES

Agopyan V., Savastano H., John V. M., Cincotto M. A. 2005. Developments on vegetable fibre-cement based materials in Sao Paolo, Brasil: an overview, Cem Concr Compos 27 (5) 527-536.

Akers S. A. S., Studinka J. B. 1989. Ageing behaviour of cellulose fibre cement composites in natural weathering and accelerated tests, The International Journal of Cement Composites and Lightweight Concrete 11 (2) 93-97.

Akers S. A. S. 1989 Micromechanical studies of fresh and weathered fibre cement composites, The International Journal of Cement Composites and Lightweight Concrete 11 (2) 117-131.

Ambrožič M., Vidovič K. 2007. Reliability of the Weibull analysis of the strength of construction materials, J Mater Sci 42 9645-9653.

Anton N., Ruiz-Prieto J. M., F. Velasco, J. M. Torralba. 1998. Mechanical properties and wear behaviour of ceramic matrix composites based on clinker portland doped with magnesia, J Mater Processing Tech 78 12-17.

Beaudoin J. J. 1990. Handbook of Fiber-Reinforced Concrete – Principles, Properties, Developments and Applications, Noyes Publications, New Jersey, US.

Caliskan S. 2003. Aggregate/mortar interface: influence of silica fume at the micro- and macro-level, Cem Concr Compos 25 (4-5) 557-564.

Cooke A. M. 2005. The measurement and significance of green sheet properties for the properties of hardened fibre cement, Cem Concr Compos 27 604-610.

Coutts R. S. P. 2005. A review of Australian research into natural fibre cement composites, Cem Concr Compos 27 (5) 518-526.

DIN 274/1. 1972. Asbestzement-Wellplatten – Masse, Anforderungen, Prufungen, April 1972.

EN 494. 2004. Fibre-cement profiled sheets and fittings for roofing – Product specification and test methods, December 2004.

Huang J . S., Cheng C. K. 2004. Fracture toughness variability of foamed alumina cements, Cem Concr Res 34 (5) 883-888.

Johnson L. G. 1951. The median ranks of sample values in their population with an application to certain fatigue studies, Industrial Mathematics 2.

Kosmač T., C. Oblak, P. Jevnikar, N. Funduk, L. Marion. 1999. The effect of surface grinding and sandblasting on flexural strength and reliability of Y-TZP zirconia ceramic, Dental Mater 15 426-433.

Lewis G., van Hooy-Corstjens C. S. J., Bhattaram A., Koole L. H. 2005. Influence of the radiopacifier in an acrylic bone cement on its mechanical, thermal, and physical properties: Barium sulfate-containing cement versus iodine-containing cement, J. Biomed Mater Res B 73B (1) 77-87.

Li G. Q., Cao H., Li Q. S., Huo D. 1993. Theory and its Application of Structural Dynamic Reliability, Earthquake Press, Beijing.

Li Q. S., Fang J. Q., Liu D. K., Tang J.2003. Failure probability prediction of concrete components, Cem Concr Res 33 (10) 1631-1636.

Lloyd D. K., Lipow M. 1962. Reliability: Management, Methods and Mathematics, Prentice Hall, Englewood Cliffs, New Jersey.

Ma Y. P., Zhu B. R., Tan M. H. 2005. Properties of ceramic fiber reinforced cement composites, Cem Conc Res 32 (2) 296-300.

Negro C., Blanco A., Fuente E., Sanchez L. M., Tijero J. 2005. Influence of flocculant molecular weight and anionic charge on flocculation behaviour and on the manufacture of fibre cement composites by the Hatschek process. Cem Concr Res 35 (11) 2095-2103.

Negro C., Blanco A., Pio I. S., Tijero J. 2006. Methodology for flocculant selection in fibre-cement manufacture, Cem Concr Compos 28 (1) 90-96.

Peled A., Mobasher B. 2005. Pultruded fabric-cement composites, ACI Mater J 102 (1) 15-23.

Purnell P., Beddows J. 2005. Durability and simulated ageing of new matrix glass fibre reinforced concrete, Cem Concr Compos 27 (9-10) 875-884.

Quinn G. 1990. Flexure strength of advanced structural ceramics: A round robin, J Am Ceram Soc 73 (8) 2374-2384.

ReliaSoft's Weibull ++. 1992. Life Data Analysis Reference, ReliaSoft Publishing.

Ritter J. E., Bandyopadhyyay N., Jakus K. 1981. Statistical reproducibility of dynamic and static fatigue experiments, Ceram Bullet 60 798-806.

Savastano H., Warden P. G., Coutts R. S. P. 2003. Potential of alternative fibre cements as building materials for developing areas, Cem Concr Compos 25 (6) 585-592.

Setien V. J., Armstrong S. R., Wefel J. S. 2005. Interfacial fracture tougness between resin-modified glass ionomer and dentin using three different surface treatment, Dent Mater 21 (6) 498-504.

Studinka J. B. 1989. Asbestos substitution in the fibre cement industry, The International Journal of Cement Composites and Lightweight Concrete 11 (2) 73-78.

Toutanji H. A. 1999. Evaluation of the tensile strength of cement-based advanced composite wrapped specimens, Comp Sci Tech 59 (15) 2261-2268.

Vidovič K., Lovreček B., Hraste M. 1996. Influence of surface charge on sedimentation and filtration behaviour of fibrous material, Chem Biochem Eng Q 10 (1) 33-38.

Weibull W. 1949. A statistical representation of fatigue failure in solids, Transactions of the Royal Institute of Technology, No. 27, Stockholm.

Weibull W. 1951. A statistical distribution function of wide applicability, J Appl Mech 18 293-297.

Wu D., Zhou J., Li Y. 2006. Unbiased estimation of Weibull parameters with the linear regression method, J Eur Ceram Soc 26 1099-1105.